scientific reports



OPEN

Propolis-loaded liposomes (ProLip) enhance macrophage-mediated immunomodulation and suppress breast cancer cell proliferation

Hamidah Mohd Zain¹, Musthahimah Muhamad¹ & Nik Nur Syazni Nik Mohamed Kamal¹,2⊠

Propolis, a natural remedy derived from bee by-products, is known for its immunomodulatory and anticancer properties. However, its clinical application is hindered by poor solubility and bioavailability. This study formulated a propolis-loaded liposome (ProLip) using the thin-film hydration technique (soy phospholipid-to-cholesterol ratio 6:1) to enhance its therapeutic effect. Encapsulation reduced the particle size of propolis from 402.77 ± 7.53 nm to 249.67 ± 5.79 nm and enhanced physicochemical properties, including a low polydispersity index (0.098 ± 0.02), highly negative zeta potential (-50.80 ± 0.10 mV), and improved solubility (water contact angle of 50.247°). FTIR analysis confirmed intermolecular interactions between phenolic groups in propolis and phospholipid carbonyl groups, while electron microscopy and surface morphology analysis revealed uniform structure and phagosomal localization in macrophages. Functionally, ProLip enhanced anti-inflammatory cytokine secretion (IL-10: 49.429 ± 0.38 pg/mL; IL-6: 40.488 ± 0.10 pg/mL) and suppressed pro-inflammatory mediators (TNF-α and IL-1β) by >80%, indicating immunoregulatory potential. Electron microscopy confirmed ProLip internalization within macrophage endocytic compartments and reduced macrophage morphological damage compared to unencapsulated propolis, validating targeted delivery and protection capacity. Additionally, conditioned media from ProLip-treated macrophages significantly induced apoptosis (>50%) and inhibited migration and invasion in MCF-7 breast cancer cells, supporting immune-mediated anticancer effects. These findings highlight ProLip's potential as a nanocarrier to enhance the bioavailability, cellular targeting, and therapeutic efficacy of stingless bee propolis in cancer immunotherapy.

Keywords Propolis, Liposome, Targeted delivery, Immunomodulation, Anti-cancer

Immunotherapy has revolutionized cancer treatment by offering innovative solutions to the challenges posed by conventional regimens such as systemic toxicity, limited efficacy, and resistance development^{1,2}. Among these strategies, immunomodulation-based therapies harness the host immune system to selectively target and eliminate cancer cells³. Macrophages, as central regulators of immune responses and the tumor microenvironment, are particularly promising targets for these therapies^{4,5}. However, the limitations of existing approaches underscore the need for novel therapeutic agents that are both effective and specific.

Propolis, a natural resinous product produced by bees, has garnered attention for its potent anti-inflammatory, antioxidant, and anticancer properties^{6–8}. Propolis derived from *Heterotrigona itama (H. itama)* stingless bees is particularly rich in phenolic and flavonoid compounds, which confer its pharmacological activity^{9,10}. Despite its promise, the clinical application of propolis remains limited due to poor water solubility, low bioavailability, and variability in chemical composition^{11,12}. These challenges have hindered its consistent therapeutic outcomes and broader adoption in oncology and immunotherapy. Moreover, mechanistic insights into its interaction with immune cells, particularly macrophages, remain underexplored, creating a critical gap in its translation to clinical applications.

Nanotechnology offers a transformative approach to address these limitations. Liposomal encapsulation, leveraging biocompatible phospholipid bilayers, can enhance the solubility, stability, and bioavailability of hydrophobic compounds such as propolis^{13,14}. This study introduces ProLip, a novel liposomal formulation

¹Department of Toxicology, Advanced Medical and Dental Institute, Universiti Sains Malaysia, Kepala Batas 13200, Penang, Malaysia. ²Breast Cancer Translational Research Program (BCTRP@IPPT), Advanced Medical and Dental Institute, Universiti Sains Malaysia, Kepala Batas 13200, Penang, Malaysia. [™]email: niksyazni@usm.my

of *H. itama* propolis, engineered to overcome the solubility barrier and improve its interaction with immune cells. ProLip not only protects the bioactive components of propolis but also facilitates efficient macrophage uptake, enabling targeted delivery and controlled release. This dual-targeted system amplifies propolis's immunomodulatory and anticancer effects, addressing the limitations of conventional therapies and current propolis-based studies.

The novelty of this work lies in its exploration of ProLip's dual therapeutic potential: modulating immune responses and inhibiting cancer progression. Unlike previous studies that focus exclusively on either immunomodulation or anticancer activity, this research investigates the synergistic interplay between these mechanisms. By combining natural bioactive with advanced nanotechnology, this study addresses critical challenges in drug delivery, immune modulation, and cancer therapy. ProLip exemplifies a novel therapeutic strategy capable of overcoming the limitations of traditional propolis formulations, offering enhanced solubility, stability, and targeted delivery. The findings not only highlight the clinical relevance of liposomal propolis but also establish its potential as a multifunctional nanotherapeutic for inflammation-driven diseases and cancer. This research provides a foundation for future studies to translate natural product-based therapies into clinical applications, bridging the gap between laboratory research and real-world healthcare needs.

Results

Physicochemical analysis and performance assessment of ProLip

The encapsulation of Pro into Lip demonstrated significant changes in the physicochemical characteristics of the ProLip formulation. Based on Fig. 1a, a significant reduction in the average particle size of Pro was observed after encapsulation into the liposomal carrier, which was from 402.77 ± 7.53 nm to 249.67 ± 5.79 nm. All samples exhibited monodisperse distribution of particles with PDI values < 0.12 (Fig. 1b). Surface charge determination, through zeta potential measurement showed an overall negative value with Lip and ProLip possessed more negative zeta potential at -51.37 \pm 1.11 mV and - 50.80 \pm 0.10 mV respectively compared to Pro alone (-1.49 \pm 0.11 mV) as observed in Fig. 1c. The degree of wettability of ProLip revealed a lower contact angle (50.247° \pm 2.76) after encapsulation compared to before encapsulation (Pro: 81.629° \pm 3.16), reflecting enhanced solubility (Fig. 1d). The in vitro release profile (Fig. 1e) showed sustained release from ProLip, reaching ~60% over 24 h, whereas Pro exhibited a rapid initial release (~98%) and Lip showed negligible release (<5%). The loading capacity (LC) and encapsulation efficiency (EE) of ProLip demonstrated high loading (72.98 \pm 0.72%) and encapsulation (83.52 \pm 0.66%) of Pro into Lip (Fig. 1f). The overall physicochemical data, including batch-to-batch reproducibility expressed as coefficient of variation (CV), are summarized in Supplementary Table S1.

Surface morphology of ProLip via SEM

The surface morphological evaluation of Pro, Lip, and ProLip was visualized by SEM analysis (Fig. 2). Based on the results, Pro exhibited an irregular circular morphology with a rough surface and heterogeneous particle sizes (Fig. 2a). In contrast, the propolis-free liposome (Lip) displayed a nearly circular smooth surface with well-defined, uniform particles (Fig. 2b). The ProLip formulation maintained a comparable uniformity in particle size but exhibited a slightly textured surface, differentiating it from the smoother morphology of Lip (Fig. 2c).

Chemical interaction of ProLip via FTIR spectra

The interaction between Pro, Lip, and ProLip were observed through the distinct changes in the peaks and intensities, as depicted in Fig. 3. According to the results, identical bands were identified in both Pro and ProLip at 3308 cm $^{-1}$, corresponding to O-H stretching. However, there was a reduction in the intensity of ProLip, characterized by a broader absorption band. Additionally, C-H stretching vibrations at 2924 cm $^{-1}$ and 2848 cm $^{-1}$ were present in all samples, with a more pronounced peak similarity between Pro and ProLip. Further spectral shifts were observed in Lip and ProLip, particularly with the presence of carbonyl (C=O) stretching at 1737 cm $^{-1}$, carboxyl (C=C) stretching at 1638 cm $^{-1}$, and aromatic C-H bending at 1446 cm $^{-1}$. In addition, a distinct O-H bending was observed at 1400 cm $^{-1}$ in Lip and 1365 cm $^{-1}$ in ProLip. The characteristic peaks of Pro at 1065 cm $^{-1}$ (C-O), 981 cm $^{-1}$ (C=C), and 795 cm $^{-1}$ (C=C) were also detected in ProLip.

Immunomodulatory activities in THP-1 macrophages

The effects of ProLip and associated controls, including Pro and Doxorubicin, were evaluated on selected biomarkers involved in immune response by ELISA assay (Fig. 4). LPS was added in the subsequent assays as it acts as a potent inflammatory stimulus¹⁵. In this assay, LPS served as an inflammatory stimulus to assess the response of PMA-differentiated THP-1 macrophages to ProLip and the associated controls. When exposed to LPS, PMA-differentiated THP-1 macrophages, similar to primary macrophages, activated signalling pathways that led to the production of pro-inflammatory cytokines, such as TNF- α and IL-1 β ^{16,17}. Supporting this, the study demonstrated that LPS enhanced the expression of TNF- α (154.54 pg/mL, ***p<0.001) and IL-1 β (231.37 pg/mL, ***p<0.001) in PMA-differentiated THP-1 macrophages, as illustrated in Fig. 4a,b, respectively.

Figure 4a illustrates the expression of TNF-α cytokine in PMA-differentiated THP-1 macrophages following treatment with ProLip and the respective controls. Following 24 h incubation with ProLip + LPS, TNF-α levels were reduced by 20.48 pg/mL relative to the LPS-treated macrophages (154.54 pg/mL, ***p<0.001). Similar findings were observed in THP-1 macrophages treated with ProLip without LPS stimulation, where TNF-α cytokine expression was measured at 30.26 pg/mL. These results indicate that ProLip suppresses the production of this key pro-inflammatory cytokine. Meanwhile, Pro and Doxorubicin treatments resulted in TNF-α cytokine expression levels of 46.13 pg/mL and 75.12 pg/mL, respectively.

Figure 4b illustrates the expression of IL-1 β cytokine in THP-1 macrophages following treatment with ProLip treatment and the respective controls. IL-1 β is a pro-inflammatory cytokine, and its elevated levels have been associated with various inflammatory diseases, including rheumatoid arthritis and the development of

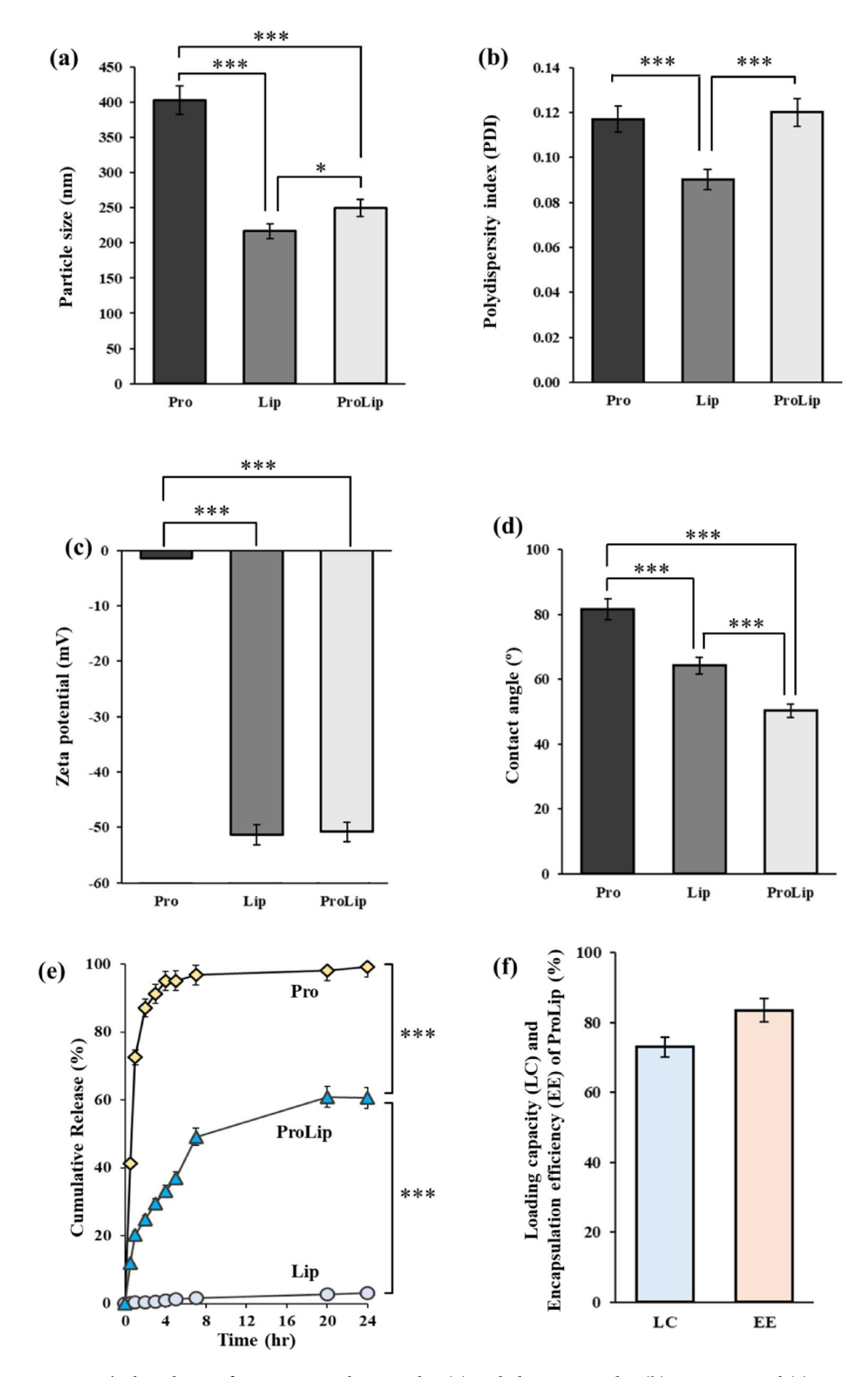


Fig. 1. The bar charts of average particle size value (a), polydispersity index (b), zeta potential (c), contact angle (d), in vitro cumulative release profile (e), and loading capacity (LC) and encapsulation efficiency (EE) of ProLip (f). Data were presented as mean \pm SD (n = 3), with statistical significance indicated as *p < 0.05, **p < 0.01, ***p < 0.001.

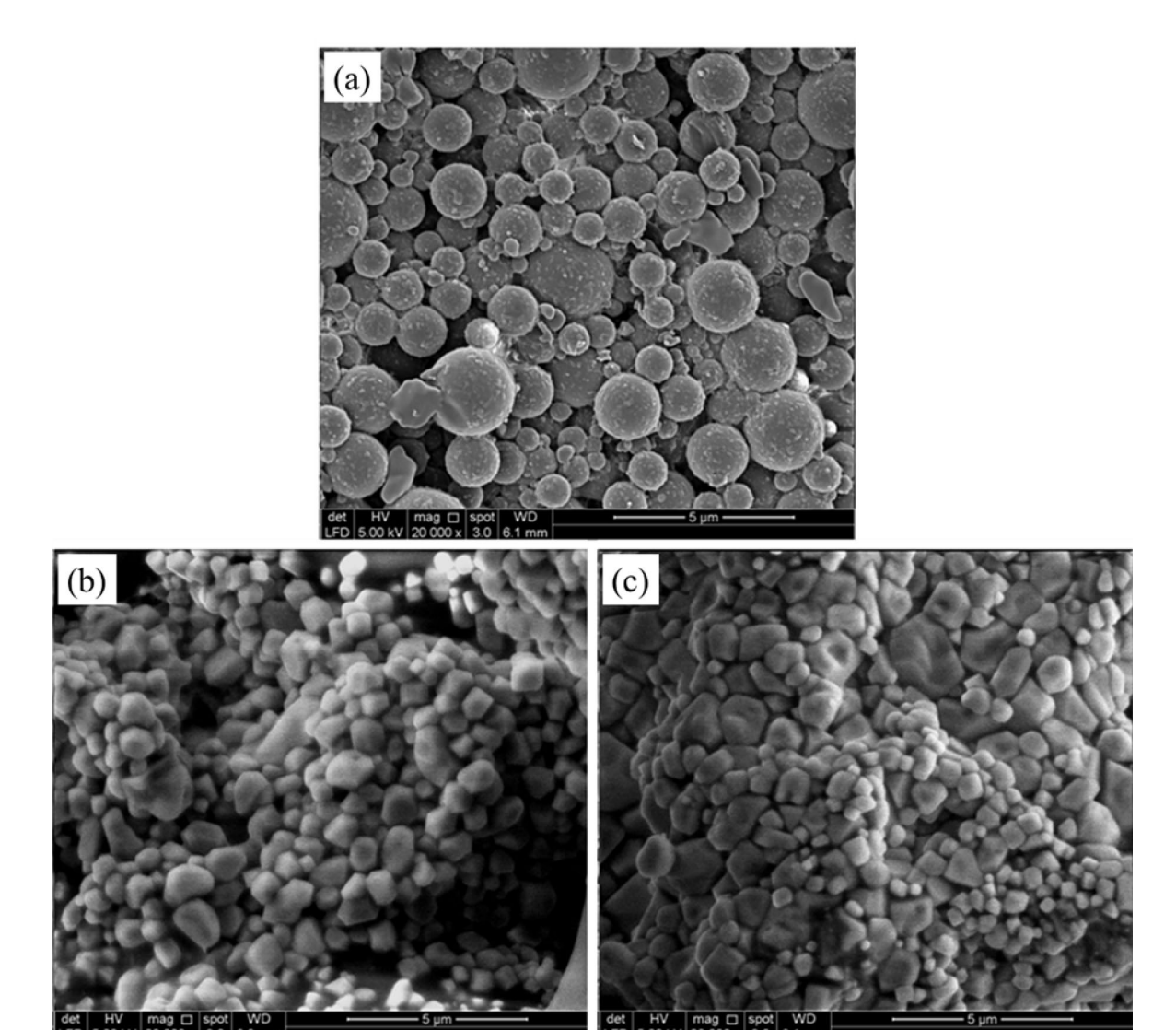


Fig. 2. Morphological visualization of (a) Pro, (b) Lip, and (c) ProLip under SEM at a magnification of 20,000x. Scale bar: 5 µm.

cancer 18 . Treatment with ProLip + LPS led to a significant reduction in IL-1 β production to 14.94 pg/mL in THP-1 macrophages compared to the LPS-treated macrophages (231.37 pg/mL, ***p < 0.001). Similar findings were observed in THP-1 macrophages treated with ProLip without LPS stimulation, where IL-1 β cytokine expression was measured at 30.46 pg/mL. This suggests that ProLip may exert an anti-inflammatory effect by suppressing the production of this key pro-inflammatory cytokine. Meanwhile, Pro and Doxorubicin treatments resulted in IL-1 β cytokine expression levels of 61.89 pg/mL and 98.03 pg/mL, respectively.

Figure 4c illustrates the expression of IL-10 cytokine in THP-1 macrophages following treatment with ProLip treatment and the respective controls. IL-10 is an anti-inflammatory cytokine produced by a variety of immune cells, including macrophages, T cells, B cells, and dendritic cells¹⁹. Treatment with ProLip resulted in an increase in IL-10 production (13.46 pg/mL, **p < 0.01) in THP-1 macrophages compared to LPS-treated macrophages (8.67 pg/mL). Comparable results were obtained in THP-1 macrophages treated with ProLip under LPS stimulation, where IL-10 levels were measured at 49.43 pg/mL (***p < 0.001). Based on these findings, it is hypothesized that ProLip may promote the anti-inflammatory function of IL-10 of THP-1 macrophages by reducing excessive inflammation in an already activated pro-inflammatory environment, as evidenced by the LPS-induced response. Meanwhile, Pro and Doxorubicin treatment resulted in IL-10 expression levels of 9.98 pg/mL and 4.16 pg/mL, respectively.

Figure 4d illustrates the expression of IL-6 cytokine in THP-1 macrophages following treatment with ProLip treatment and the respective controls. IL-6 is a pleiotropic cytokine, exhibiting both pro-inflammatory and anti-inflammatory activities depending on the specific cellular context, including the microenvironment, the presence of other cytokines, and the target cell type^{20,21}. Treatment with ProLip increased IL-6 production (24.17 pg/mL, ***p < 0.001) in THP-1 macrophages compared to LPS-treated macrophages (10.80 pg/mL). Comparable results were obtained in THP-1 macrophages treated with ProLip + LPS, where IL-6 levels were

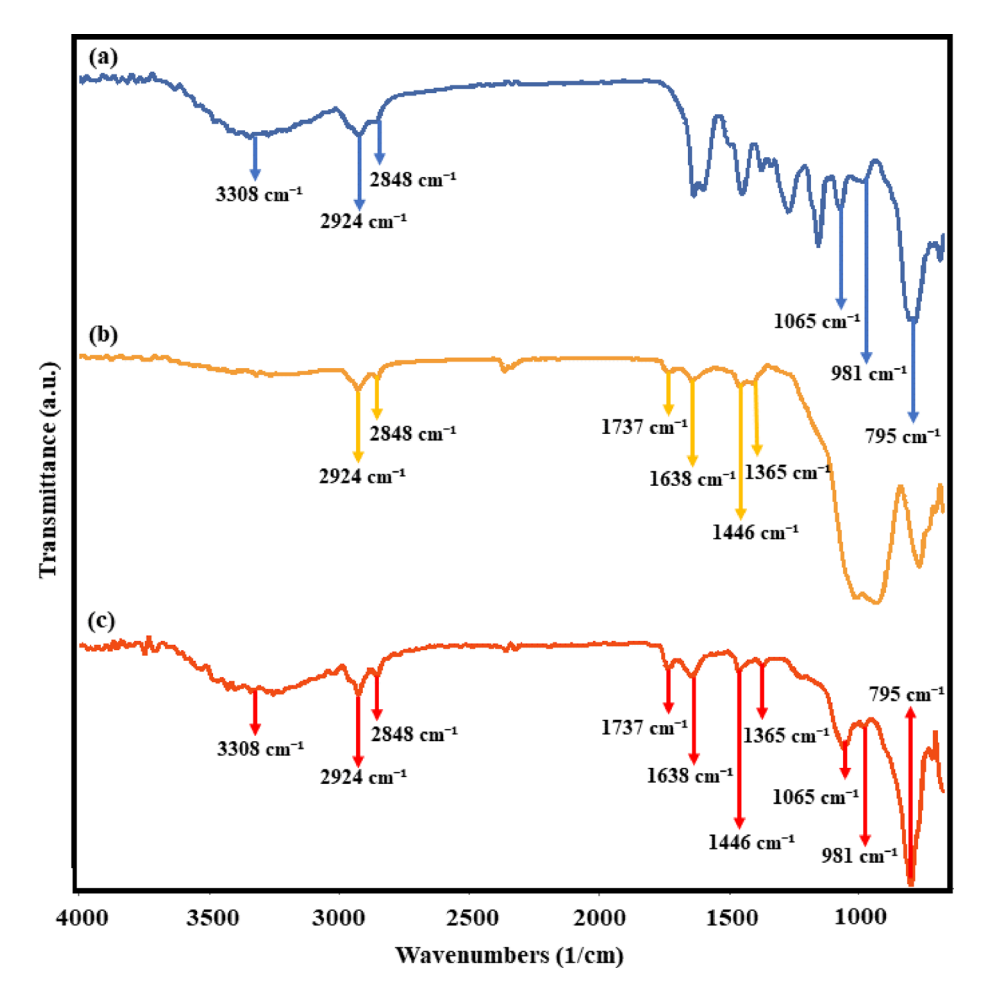


Fig. 3. Characteristic functional group variations of the FTIR spectra in (a) Pro, (b) Lip, and (c) ProLip.

measured at 40.49 pg/mL (***p<0.001). Based on these findings, it is hypothesized that ProLip may promote the anti-inflammatory function of IL-6 of THP-1 macrophages by reducing excessive inflammation in an already activated pro-inflammatory environment, as evidenced by the LPS-induced response. Meanwhile, Pro and Doxorubicin treatment resulted in IL-6 expression levels of 12.58 pg/mL and 7.13 pg/mL, respectively.

Morphological analysis of ProLip uptake

The intracellular localization and morphological changes induced by Pro and ProLip in THP-1 macrophages, both in the presence and absence of LPS, were conducted by TEM analysis. As shown in Fig. 5, untreated (UT) THP-1 macrophages exhibited a healthy and viable cellular structure, characterized by intact organelles, a large nucleus with well-defined chromatin, abundant mitochondria, and an intact plasma membrane (Fig. 5B(i-ii))^{23,24}. Macrophages, being phagocytic cells, engulf foreign materials such as Pro, encapsulating them within a membrane-bound vesicle known as a phagosome. As depicted in Fig. 5C(i-ii), Pro was found inside phagosomes. The phagosome usually fuses with lysosomes to form phagolysosome, where the engulfed material undergoes enzymatic degradation and digestion²⁵. This process may explain the presence of electron-dense propolis-like material within the macrophage cytoplasm, likely due to phagolysosomal membrane disruption or passive diffusion following degradation²⁶, leading to the release of Pro into the cytoplasm.

The presence of larger vesicles, likely phagosomes, indicated that phagocytosis was the primary uptake mechanism of ProLip by THP-1 macrophages (Fig. 5D (i-ii)). This observation was further supported by pseudopod-like structures surrounding the large vesicles, suggesting active phagocytosis. These structures likely represented the macrophage membrane extending and enclosing the ProLip during the engulfment process. No free ProLip was detected in the cytoplasm; it was only found within phagocytic vacuoles.

LPS is a potent immunostimulant that activates THP-1 macrophages, resulting in enhanced phagocytic activity and increased lysosomal enzyme production²⁷. Lysosomes have the ability to fuse with the plasma membrane, resulting in the extracellular release of their contents²⁸. This can occur as part of a cellular response to inflammation, potentially exacerbated by LPS stimulation. The combined challenge of Pro and LPS may exert an overwhelming impact, potentially leading to macrophage cell death (cytotoxicity) and the subsequent release of lysosomal and cytoplasmic contents, as depicted in Fig. 5E(i-ii).

Interestingly, ProLip was exclusively located within membrane-bound vesicles, phagosomes, even in the presence of LPS stimulation (Fig. 5F(i-ii)). Similar to ProLip alone, no free ProLip+LPS was detected in the

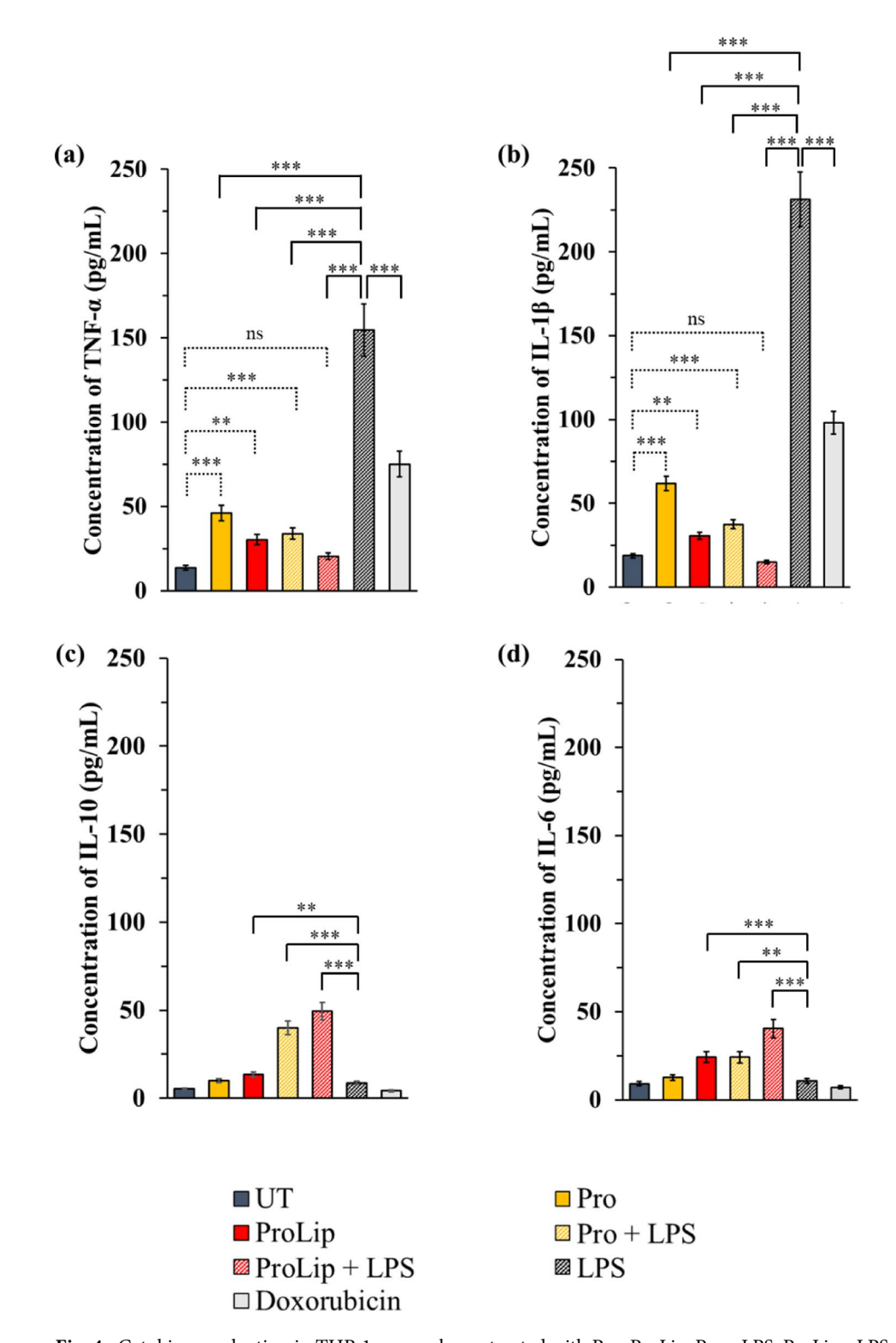


Fig. 4. Cytokine production in THP-1 macrophages treated with Pro, ProLip, Pro + LPS, ProLip + LPS, LPS, and Doxorubicin. (a) TNF-α, (b) IL-1β, (c) IL-10 and (d) IL-6 levels were quantified. Data was presented as mean \pm SD (n = 3). Statistical analysis was analysed using one-way ANOVA followed by Tukey's post hoc test (*p < 0.05; ns = not significant, **p < 0.01, ***p < 0.001).

macrophage cytoplasm. These findings suggest efficient containment and processing. Liposomes are commonly utilized as a drug and nanoparticle carrier due to their biocompatibility and efficient uptake by macrophages through phagocytosis²⁹. Liposomal encapsulation likely enhanced ProLip uptake compared to free Pro. As reported by Marrocco & Ortiz (2022), LPS stimulation can enhance macrophage activity, which may contribute

to the observed synergistic effect of liposomal delivery under LPS exposure in facilitating the efficient engulfment of ProLip within phagosomes³⁰.

Figure 5G(i-ii) depicts THP-1 macrophages under LPS exposure. It was observed that activated macrophages underwent morphological changes, becoming larger and flatter. The cell membrane formed ruffles and extensions, known as filopodia^{31,32}. These dynamic membrane protrusions play a crucial role in capturing and engulfing pathogens and other targets³³. Figure 5H(i-ii) presents a TEM micrograph of a THP-1 macrophage after exposure to Doxorubicin. As observed, different stages of phagosomes and lysosomes were present, and some Doxorubicin appeared to have escaped the phagocytic pathway, dispersing throughout the macrophage cytoplasm and accumulating on the outer layer of the phagosome/lysosome membrane.

Adjuvant activity and effect on breast cancer cells

Building on the observed effects of Pro and ProLip, conditioned media from Pro, ProLip, and other treated macrophages (including Pro+LPS, ProLip+LPS, LPS, and Doxorubicin) were investigated on MCF-7 breast cancer cells (Fig. 6). It was hypothesized that ProLip modulated macrophage activity, which in turn impacted the behavior of neighbouring breast cancer cells. This co-culture assay aimed to characterize the interactions between ProLip-treated macrophages and breast cancer cells, focusing on migration and invasion activities, as well as mechanisms of cell death.

Before performing the co-culture assays, the direct cytotoxicity of ProLip on MCF-7 cells was quantified using the 3-(4,5-dimethylthiazol-2-yl)-2,5-diphenyltetrazolium bromide (MTT) assay across a concentration range of 0–250 μ g/mL. The concentration selected for the co-culture assays (50.35 μ g/mL) corresponded to a sub-cytotoxic dose, maintaining approximately 70% cell viability (mean \pm SD) after 24 h of exposure, thereby confirming that the cells remained largely viable. Accordingly, the anti-tumor effects observed in the co-culture system are likely to be primarily immune-mediated rather than attributable to direct cytotoxicity induced by ProLip alone.

Based on the results, treatment with Pro, ProLip, Pro + LPS, and ProLip + LPS macrophage conditioned media exhibited a pronounced suppression of MCF-7 cells' migration after a 24-hr incubation, with minimal wound closure observed as compared to the baseline scratch area at 0 h (Fig. 6c,d). In contrast, the untreated control group (UT) and Doxorubicin showed nearly complete wound closure by 24 h. LPS -conditioned media group, in particular, showed a gradual migration after 24 h, in comparison to the control. Meanwhile, the Transwell invasion assay demonstrated that treatment with Pro and ProLip significantly inhibited MCF-7 invasion compared to the untreated control, 16.77% (***p<0.001) and 11.38% (***p<0.001), respectively (Fig. 6e,f). The inhibitory effect was further enhanced in the presence of LPS. Specifically, Pro + LPS reduced invasion by 10.21% compared to the UT control, while ProLip + LPS exhibited the most pronounced reduction, decreasing invasion by 7.98%. While the effects of LPS alone and Doxorubicin were less pronounced compared to ProLip and the combination treatments, the results demonstrated a 63.31% (***p<0.001) and 73.58% (**p<0.01) reduction in invasion, respectively, compared to the untreated cells.

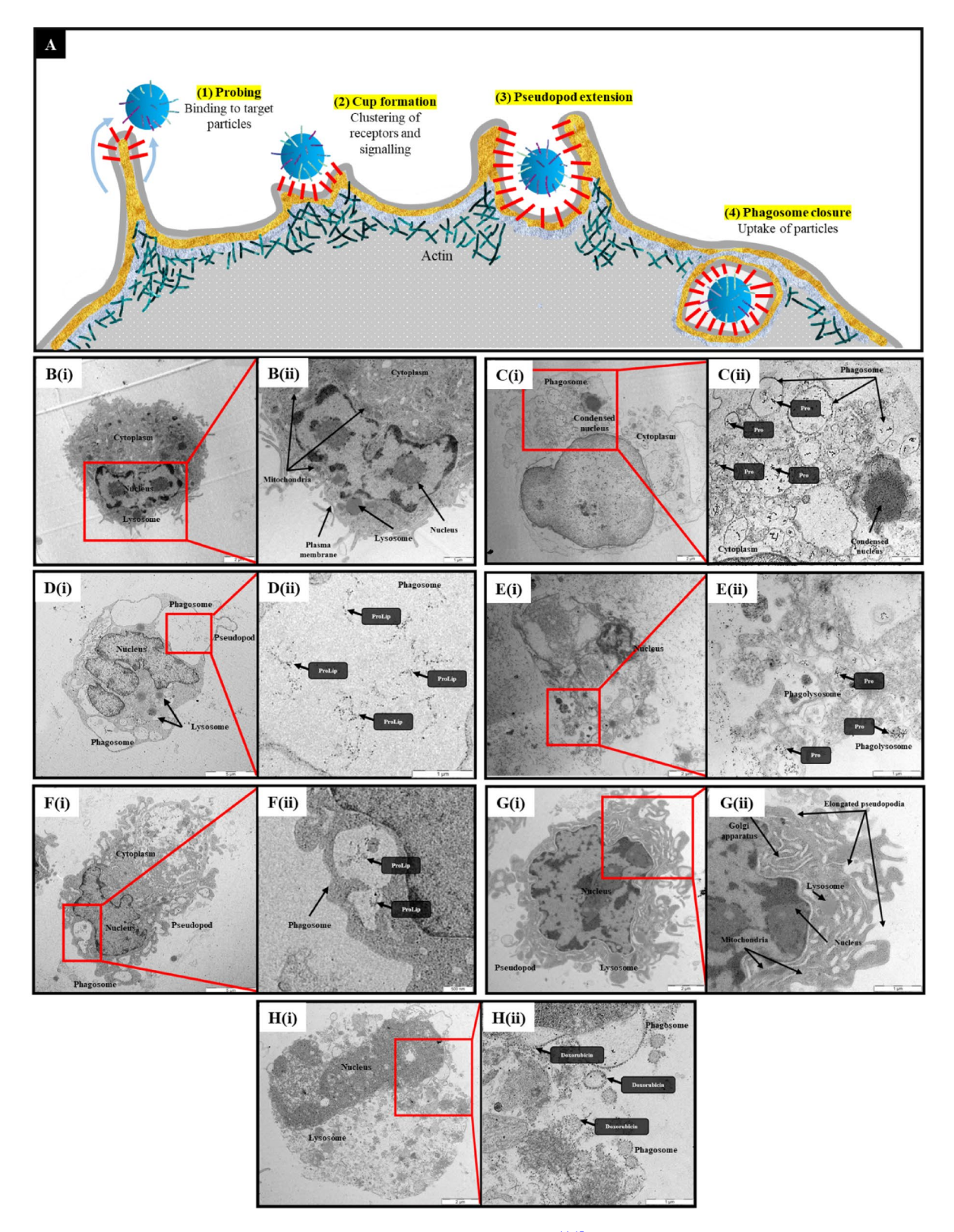
As for cell death mechanism, MCF-7 cells treated with Pro-macrophage conditioned media showed a significant increase, in which $38.56\% \pm 2.58$ (***p<0.001) of cells underwent apoptotic cell death compared to the untreated control cells observed (Fig. 6a,b). Interestingly, apoptosis was significantly higher in MCF-7 cells following incubation with ProLip-macrophage conditioned media, reaching 55.83% (***p<0.001). Under LPS stimulation, treatment with Pro- and ProLip macrophage conditioned media resulted in a significant increase in apoptotic cell death in MCF-7 cells, reaching 47.41% (***p<0.001) and 69.36% (***p<0.001), respectively. In contrast, conditioned media from LPS alone or the chemotherapeutic agent doxorubic in induced lower levels of apoptosis in MCF-7 cells, with $13.07\% \pm 4.02$ and $28.56\% \pm 2.21\%$ of apoptotic cells, respectively.

Discussion

This study presents a comprehensive integration of nanotechnology with natural immunotherapy by employing liposomal encapsulation of propolis (ProLip), aiming to overcome the physicochemical limitations of crude propolis (Pro) and enhance its biological efficacy in modulating immune cell behavior. Propolis, a resinous natural product from bees, is widely recognized for its potent anti-inflammatory and anticancer properties; however, its clinical translation has been limited by poor aqueous solubility, instability, and reduced bioavailability^{34,35}. These challenges significantly affect its cellular uptake and therapeutic consistency. Our findings demonstrate that the physicochemical modifications achieved through liposomal encapsulation significantly improved the bioavailability, stability, and cellular interaction of propolis. Crude propolis, when directly exposed to cells, exhibited uncontrolled cytotoxicity and induced cellular stress, likely due to its non-specific interaction with cellular membranes and tendency to form intracellular aggregates, as previously reported^{36–38}. By encapsulating propolis in liposomes, these challenges were effectively mitigated.

The ProLip formulation displayed enhanced hydrophilicity and uniform dispersion of propolis within the liposomal bilayer, transforming the aggregated resinous particles of crude Pro into a stable nanosystem. This reconfiguration significantly improved delivery characteristics, as evidenced by the mean particle size of 249.67±5.79 nm, an optimal size range for cellular uptake via endocytosis and enhanced accumulation at sites of inflammation or tumorigenesis^{39,40}. Nanosized particles within this range are known to exhibit prolonged systemic circulation and enhanced permeability and retention (EPR) effects, facilitating passive targeting of inflammatory tissues and tumors^{41,42}. Furthermore, macrophages are highly phagocytic and naturally internalize nanoparticles within this size spectrum, enabling ProLip to be preferentially taken up through actin-mediated phagocytosis and macropinocytosis⁴³.

The ProLip formulation also exhibited a highly negative zeta potential $(-50.80\pm0.10 \text{ mV})$, attributed to the presence of deprotonated phenolic groups and negatively charged phospholipids. This surface charge enhanced colloidal stability through electrostatic repulsion and prevented nanoparticle aggregation, contributing to a low



polydispersity index (PDI) and uniform particle distribution^{44,45}. In addition to its role in stability, negative zeta potential has been shown to improve macrophage uptake efficiency by 5.3-fold compared to neutral liposomes⁴⁶. The hydrophilicity of ProLip, validated by contact angle measurement, further supported its suitability for biological applications. Increased wettability allowed for better interaction with aqueous biological environments, improving cell surface adherence and internalization efficiency^{47,48}. Enhanced aqueous compatibility is a critical feature for any nanoformulation targeting immune cells, particularly macrophages, which thrive in dynamic fluidic environments and regulate immune responses through both direct contact and soluble mediators⁴⁹.

FTIR and SEM analyses confirmed successful molecular integration and morphological reconfiguration of propolis within the liposomal matrix. FTIR spectra revealed spectral shifts and band broadening, particularly in

∢Fig. 5. TEM of phagocytic uptake and intracellular trafficking of treatments in THP-1 macrophages following 24 h exposure. (A) Schematic illustration of the key stages of phagocytosis. Macrophages formed an actin-mediated membrane ruffling to sense particles and initiate engulfment. Progressive pseudopod extension led to the engulfment of particles forming a phagosome. (Adapted from Moreno et al., 2022)²². (B−H) Each treatment condition is represented by two images: a low-magnification overview (left) and a high-magnification image (right) showing subcellular details. Untreated control cells showed no morphological abnormalities (B(i-ii)). Pro and ProLip were deposited within the membrane-bound structures and identified as electron-dense particles. Magnified electron micrograph showed phagolysosome containing Pro (C(ii)), ProLip (D(ii)), Pro+LPS (E(ii)), ProLip+LPS (F(ii)), and Doxorubicin (H(ii)). Activated macrophages showed extensive pseudopods and phagocytic activity (F(i-ii) and G(i-ii)). Magnification: B(i): x2000, B(ii): x4000, C(i): x2000, C(ii): x6300, D(i): x1600, D(ii): x6300, E(i): x2500, E(ii): x6300, F(ii): x1600, F(ii): x8000, G(i): x2500, G(ii): x2500, H(ii): x2500, H(ii): x6300.

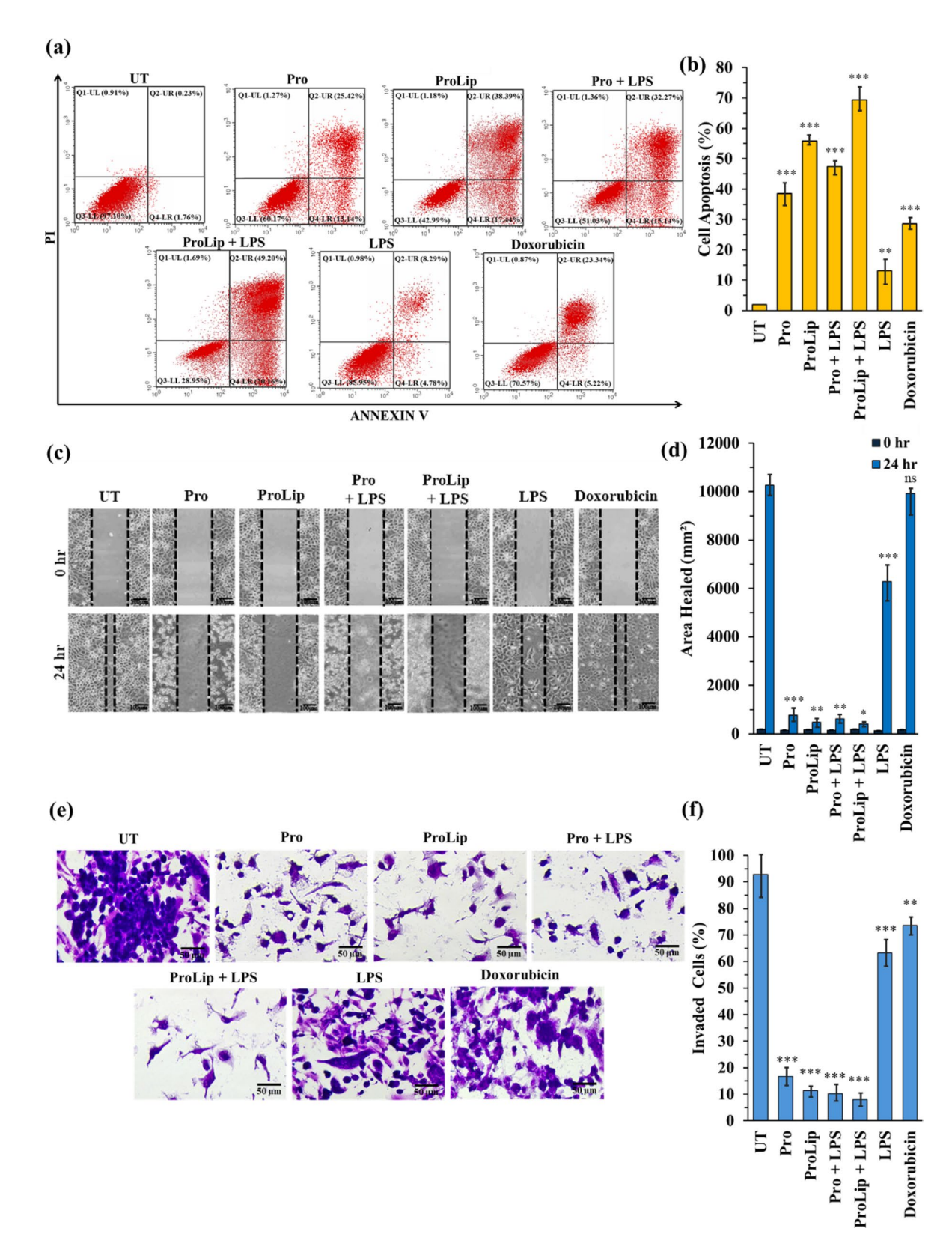
the carbonyl and hydroxyl regions, suggesting the formation of hydrogen bonding and van der Waals interactions between propolis phenolics and phospholipid components⁵⁰. These molecular interactions indicate strong compatibility between the payload (Pro) and carrier (Lip), crucial for maintaining structural integrity during circulation and ensuring controlled drug release. Meanwhile, SEM analysis revealed distinct morphological differences between ProLip and the unloaded liposome (Lip). The surface of ProLip exhibited increased roughness and slight irregularities, likely attributable to the deposition of complex organic constituents present in propolis onto the liposomal surface⁵⁰. These morphological alterations suggest effective integration of Pro within the hydrophobic domains of the lipid bilayer.

Biologically, ProLip outperformed crude Pro in terms of immunomodulatory potency and cellular compatibility. Propolis is known for its immunomodulatory properties, with its polyphenolic constituents exerting dual effects by suppressing excessive inflammation while promoting immune homeostasis^{51,52}. In this study, ELISA results revealed significantly higher levels of IL-10 and IL-6 in ProLip-treated macrophages compared with those treated with crude propolis (Pro). These findings indicate that encapsulation drove macrophages toward a pro-resolving phenotype from a pro-inflammatory state. This phenotype is marked by lower inflammatory factors and increased anti-inflammatory signaling, which favors tissue repair over persistent inflammation⁵³. Notably, the co-treatment of macrophages with ProLip and LPS elicited a synergistic increase in IL-10 and IL-6 expression, indicating the formulation's capacity to modulate macrophage activation even under pro-inflammatory stimulation^{54,55}. ProLip further demonstrated enhanced suppression of pro-inflammatory cytokines (IL-1β and TNF-α) compared with Pro, suggesting that the encapsulated formulation improves active-polyphenol bioavailability and augments modulation of inflammatory signalling pathways⁵⁶.

Nuclear factor- κB (NF- κB) represents a family of inducible transcription factors that regulate large sets of genes engaged in immune and inflammatory activities ⁵⁷. In particular, it drives the expression of pro-inflammatory cytokines such as IL-1 β , TNF- α , and IL-6 (Liu et al., 2017). NF- κB can be activated through two principal pathways, canonical and non-canonical (alternative); despite mechanistic differences, both play crucial roles in regulating immune and inflammatory responses ⁵⁷. The canonical NF- κB activation pathway begins when the I κB kinase (IKK) complex, composed of IKK α , IKK β , and regulatory subunit NEMO, is activated by a signal ^{58,59}. The IKK complex then phosphorylates the inhibitory protein I $\kappa B\alpha$ at specific sites, triggering its ubiquitination and degradation by the 26 S proteosome. This degradation releases the NF- κB transcription factor, allowing it to translocate to the nucleus and initiate the transcription of target genes that promote immune and inflammatory responses ^{60,61}. Targeting the NF- κB pathway is a promising strategy because its dysregulated activation is a common driver of inflammatory, neoplastic, and autoimmune diseases ^{58,62,63}. This aberrant signaling influences key processes, including inflammation, cell proliferation, survival, and metastasis ^{59,64,65}.

IL-10, on the other hand, is an anti-inflammatory cytokine that helps to dampen the inflammatory response, often produced by macrophages themselves 66 . In response to infection, the immune system shifts towards a more pro-inflammatory state to eliminate the pathogen. Maintaining a balance between IL-10 and pro-inflammatory cytokines is critical to resolve the infection while limiting tissue damage 67,68 . In the context of NF- κ B, IL-10 suppresses this pathway, which normally drives transcription of pro-inflammatory genes such as IL- 69,70 . Mechanistically, IL-10 acts at multiple levels – it reduces I κ B kinase (IKK) activity, thereby limiting NF- κ B activation, and it impairs NF- κ B binding to DNA 71,72 . This, in turn, downregulates pro-inflammatory mediators, promoting resolution of inflammation and supporting tissue survival. Taken together, these findings highlight ProLip's therapeutic potential to balance between immunostimulation and immunosuppression, supporting its development as a versatile immunotherapeutic agent 73 .

TEM imaging provided further insight into the intracellular behavior of Pro and ProLip. While Pro formed irregular and undefined aggregates in the cytoplasm, causing structural disruption to cellular organelles, ProLip was internalized more uniformly and trafficked toward lysosomal and phagosomal compartments. ProLip preserved membrane integrity and mitochondrial structure, suggesting that liposomal encapsulation shielded macrophages from potential damage while retaining propolis's biological activity³⁶. This behavior indicates that the encapsulation of Pro within liposomes likely facilitated its uptake through endocytic pathways, particularly clathrin- and caveolin-mediated endocytosis, mechanisms commonly observed in liposomal drug delivery systems^{74,75}. By preventing premature degradation and enabling sustained intracellular release, ProLip's encapsulation enhances bioavailability and mitigates cytotoxic stress²⁹. The preferential localization within lysosomal compartments suggested that macrophages actively processed and degraded ProLip, allowing for sustained intracellular release of bioactive compounds. In comparison, doxorubicin, a commonly used chemotherapeutic, demonstrated widespread intracellular dispersion and nuclear condensation, confirming its



passive diffusion and DNA intercalation-based mechanism of cytotoxicity^{76,77}. These findings emphasize the difference in cellular handling between synthetic drugs and biologically encapsulated therapeutics like ProLip. While doxorubicin causes significant genotoxic stress, ProLip achieved effective intracellular delivery without inducing similar levels of cellular damage.

To further assess the therapeutic potential of ProLip, this study utilized the human monocytic cell line THP-1 as a platform to investigate the interactions between MCF-7 breast cancer cells and THP-1-derived macrophages treated with ProLip. By recreating the inflammatory condition established by stimulation with LPS, the present study aimed to determine whether ProLip enhances or mitigates the anti-tumorigenic activities of M1-like

∢Fig. 6. Representative Assessment of ProLip's immunomodulatory and anticancer activities in breast cancer cells using different formulations of macrophage-conditioned media. (a) Flow cytometric analysis of apoptosis in MCF-7 cells. The quadrants represent viable, early apoptotic, late apoptotic, and necrotic cell populations. (b) Quantification of apoptotic cells. ProLip enhanced apoptotic activity compared to other groups. (c) Wound healing assay of MCF-7 cells. Representative images at 0 and 24 h show reduced wound closure in ProLiptreated cells. (d) Quantification of wound healing (mm²) after 24 h. ProLip showed significant inhibition of MCF-7 cell migration compared to controls and other treatments. (e) Transwell invasion assay of MCF-7 cells. Images show reduced invasive cell numbers in ProLip-treated groups. (f) Quantification of invasive cells. UT: untreated; Pro: propolis; ProLip: propolis liposome; LPS: lipopolysaccharide. Data were presented as mean ± SD (n = 3). Statistical significance was indicated as ****p < 0.001 compared to the untreated control (UT).

macrophages within a model of the tumor microenvironment. The present study found that the conditioned media significantly inhibited MCF-7 cell migration. Consistently, results from the Transwell invasion assay demonstrated that THP-1 macrophages treated with ProLip more effectively suppressed the invasive behavior of MCF-7 cells compared to unencapsulated propolis. Interestingly, this growth inhibitory effect correlated with an increased apoptotic population in MCF-7 cells following exposure to conditioned media derived from ProLiptreated THP-1 macrophages.

Macrophages, particularly the classically activated M1 subtype, have been documented to play a key role in inducing apoptosis in cancer cells through the release of pro-inflammatory cytokines such as TNF- α and IFN- γ . These cytokines activate intracellular signalling pathways that ultimately trigger programmed cell death in cancer cells⁷⁸. Moreover, M1 macrophages are also known to possess both phagocytic and antigen-presenting capabilities, allowing them to produce pro-inflammatory cytokines and exert cytotoxic effects. Through these functions, they can directly eliminate target cells via the generation of ROS, reactive nitrogen species (RNS), IL-1 β , and TNF- α . Alternatively, M1 macrophages can also promote indirect cytotoxicity by activating other immune cells, such as NK cells and T cells⁷⁹. In the present study, exposure to ProLip significantly increased the levels of TNF- α and IL-1 β in THP-1 macrophages compared to untreated cells. This elevated production of pro-inflammatory cytokines strongly indicates that ProLip promotes a pro-inflammatory, M1-like macrophage phenotype. These findings also suggest that ProLip may enhance the cytotoxic capacity of M1 macrophages against MCF-7 breast cancer cells, either directly or indirectly, through the activation of other immune cells. Such multifaceted signalling pathways underscore TNF- α 's role as a potent anticancer cytokine⁸⁰. The dual capability of ProLip to reduce inflammation in resting macrophages while enhancing pro-inflammatory, tumor-suppressive responses in inflamed or LPS-stimulated environments underscores its adaptive immunomodulatory profile.

Taken together, these findings highlight the capacity of ProLip to modulate macrophage activity and induce apoptosis in estrogen receptor (ER)-positive breast cancer cells, supporting its potential as an immunomodulatory adjunct in breast cancer management. Despite the limitation of using only one cell line, the present study employed MCF-7 cells, which represent the most common breast cancer subtype, accounting for approximately 70% of breast carcinoma cases worldwide^{81–83}. Beyond serving as a canonical ER-positive model, MCF-7 cells exhibit phenotypic and gene expression profiles characteristics of the luminal breast lineage and share certain proliferative traits with luminal B tumors⁸⁴making them particularly suitable for exploring hormone-dependent tumor-immune interactions in a controlled context.

Although THP-1-derived macrophages do not fully recapitulate the complexity and heterogeneity of primary human macrophages, which may vary in phenotype and function depending on donor background and tissue microenvironment⁸⁵they remain a widely accepted standard model in research. THP-1 cells are a well-established human monocytic cell line that can be differentiated into macrophage-like cells with consistent and reproducible characteristics. Compared with primary macrophages, they provide greater experimental uniformity, reduced donor-to-donor variability, and are commonly used as a standardized model for investigating macrophage polarization, immune responses, and tumor-immune interactions^{86–90}. These features were particularly important for ensuring reproducibility in the co-culture system with breast cancer cells used in the present study.

The present study focuses on macrophages because they are sentinel effector cells of the mononuclear phagocyte system – a group of cells including monocytes, macrophages, and dendritic cells, originate from bone marrow progenitors⁹¹. Macrophages are a major cell population in most of the tissues in the body, their numbers increase further in inflammation, wounding and malignancy, whilst their activation sate (M1 or M2) determines their specific roles in inflammation and healing 92-94. Macrophages are widely recognized as key effector cells of the innate immune system that participate directly and indirectly in host defense against pathogens. Strategically positioned within tissues, macrophages efficiently sense danger signals⁹¹thereby justifying their selection as the primary focus of this study. Moreover, activated macrophages are recognized mediators of tissue injury, capable of inducing apoptosis through multiple mechanisms⁹⁵. In addition, focusing on a single lineage enabled mechanistic analyses using validated macrophage assays while minimizing confounding from interlineage heterogeneity. Besides, macrophages were selected as the primary platform due to their surveillance role in orchestrating early inflammatory programs and shaping downstream adaptive responses. By profiling macrophages mediators (IL-1β, IL-6, TNF-α, IL-10), the present study provides an indirect but informative window into broader immunomodulation, given their central roles in coordinating dendritic cell and T cell responses 96-98. For examples, macrophages secrete signaling molecules that recruit and activate other immune cells, modulate antigen processing and presentation, and ultimately stimulate T cells to orchestrate an adaptive immune response⁹⁶⁻⁹⁹. In turn, these findings provide a valuable window into the immune system's complex regulatory processes and open new avenues for mechanistic investigation. Nevertheless, extending analyses to other immune cell models, like dendritic cells and T cells, will broaden the scope beyond macrophage-driven responses and provide a more integrated view of the continuum between innate and adaptive immunity.

Conclusion

This study established liposomal encapsulation as a effective strategy to enhance the therapeutic potential of Heterotrigona itama propolis by addressing its physicochemical limitations and improving its biological performance. The development of ProLip significantly improved the aqueous solubility, stability, and cellular bioavailability of crude propolis, enabling efficient macrophage-targeted delivery while minimizing nonspecific cytotoxicity. Physicochemical characterization confirmed successful integration of propolis into the liposomal bilayer, resulting in a nanosized, stable formulation with enhanced hydrophilicity and favorable surface charge for immune cell interaction. Biologically, ProLip preserved and amplified the immunomodulatory properties of propolis, as evidenced by increased anti-inflammatory cytokine production and attenuation of proinflammatory mediators in THP-1-derived macrophages. Under inflammatory conditions, ProLip promoted a pro-inflammatory, M1-like macrophage phenotype that enhanced apoptosis and suppressed the migration and invasion of MCF-7 breast cancer cells, suggesting improved immunotherapeutic potential. Collectively, these findings demonstrate that liposomal encapsulation not only optimizes the pharmacological profile of propolis but also augments its functional impact on immune modulation and cancer cell suppression. These findings position ProLip as a foundation for the development of next-generation macrophage-targeted immunotherapies, with the potential to shape innovative strategies that harness immune modulation to combat breast cancer more effectively.

Materials and methods Materials

Propolis from *Heterotrigona itama* (*H. itama*) stingless bee species, was purchased from a local beekeeping company, Bayu Gagah Sdn Bhd (Kulim Hightech, Kedah, Malaysia). Soy phospholipids (≥99%, Catalog #11145-50G), phosphate-buffered saline (PBS) tablets (Catalog #P4417-50TAB), lipopolysaccharides (LPS, Catalog #L6136-25MG), and phorbol 12-myristate 13-acetate (PMA, ≥ 99%, Catalog #P8139-1MG) were acquired from Sigma-Aldrich (St. Louis, USA). Cholesterol (≥99%, Catalog #08722-81) was sourced from Nacalai Tesque (Kyoto, Japan). Methanol (≥99.9%, Catalog #1060182500) and chloroform (≥99.9%, Catalog #1070242500) were purchased from Merck Millipore (Germany). THP-1 (ATCC* TIB-202™) and MCF-7 (ATCC* HTB-222™) cells were purchased from American Type Culture Collection (ATCC*) (Porton Down, Salisbury, UK). Roswell Park Memorial Institute Medium (RPMI, Catalog #RPMI-HA), Dulbecco's Modified Eagle Medium (DMEM, Catalog #DMEM-HPSTA), Penicillin-Streptomycin (Catalog #PS-B), Fetal bovine serum (FBS, Catalog #FBS-16 A), and trypsin (Catalog #TRY-3B) were procured from Capricorn Scientific (Ebsdorfergrund, Germany). Enzyme-linked Immunosorbent assay (ELISA) kits (Catalog #E-EL-H0109, #E-EL-H0149, #E-EL-H6156, #E-EL-H6154) and apoptosis kits (Catalog #E-CK-A211) were acquired from ElabScience Biotechnology Co., Ltd (China). Transwell polycarbonate membrane cell culture inserts (Catalog #CLS3412-24EA) were purchased from Corning (Massachusetts, USA).

Preparation of propolis liposome (ProLip)

Propolis encapsulation was carried out by the thin-film hydration technique⁵⁰. A mixture of 3 mg/mL ethanolic extract of propolis (EEP) with a (6: 1) ratio of phospholipid and cholesterol was solubilised in 10 mL methanol: chloroform (1:1 v/v), followed by evaporation at 45 °C using a rotary evaporator (Buchi, USA). All organic solvents were completely removed by rotary evaporation and lyophilization prior to biological testing, ensuring that the final ProLip formulation was free from detectable solvent residues that could interfere with cell-based assays. A lipid thin film was formed and subsequently hydrated using 10 mL of phosphate-buffered saline (PBS) (10 mL), while continuously stirring at 150 rpm for 30 min. The resulting suspension of propolis liposome (ProLip) was homogenized using a QSonica ultrasonic homogenizer (Q700, USA) for 30 min at 60% amplitude on ice to prevent temperature elevation. ProLip was harvested at 9000 rpm by centrifugation for 1 h at 4 °C, washed several times, recentrifuged, and finally resuspended in PBS. The liposomal suspension was lyophilized for 72 h to obtain dried ProLip extract.

To evaluate the loading capacity (LC) and encapsulation efficiency (EE) of ProLip, calculations were performed using the following formula, as described by Herdiana and colleagues¹⁰⁰:

EE (%) = (Amount of encapsulated propolis / Initial amount of ProLip) \times 100

LC (%) = (Amount of encapsulated propolis / Weight of lyophilized ProLip) × 100

Briefly, after liposomal formulation, ProLip was appropriately collected by centrifugation at 4000 rpm for 20 min at 4 °C using a refrigerated centrifuge, enabling the separation of encapsulated propolis within the liposomes (pellet) from free, unencapsulated propolis present in the supernatant. Then, the supernatant and pellet were separately lyophilized and redissolved in distilled water to measure the optical density (OD) at 420 nm. The total flavonoid contents (TFC) in both supernatant and pellet were quantified by referencing the calibration curve constructed using standard solutions. To determine the weight of the liposomal formulations, the pellet obtained after centrifugation was lyophilized for 72 h, and the dried samples were weighed using a precision analytical balance. All measurements were performed in triplicate to ensure reliability and reproducibility of the data.

Determination of particle size, polydispersity index (PDI), and zeta potential of ProLip

The particle size, polydispersity index (PDI), and zeta potential of the liposomal formulations were measured using a Zetasizer (Ver. 7.11, Malvern Instruments, Worcestershire, UK). For these measurements, a small

amount of the liposomal suspension was redispersed in deionized water and sonicated briefly to ensure uniform dispersion. The particle size and PDI were determined using dynamic light scattering (DLS), while the zeta potential was measured through electrophoretic light scattering (ELS). Measurements were performed in triplicate.

Measurement of dynamic contact angle

Dynamic contact angle measurements were performed using the DataPhysics DCAT21 (DataPhysics Instruments GmbH, Germany) to assess the wettability of propolis after its encapsulation into a liposomal nanocarrier. Powder contact angle measurements were conducted for propolis (Pro), while solid contact angle measurements were carried out for the liposome (Lip) and ProLip formulations. For the powder measurement, 400 mg of Pro was weighed and compressed into a sample glass tube. Calibration was performed using hexane as the reference liquid. For the solid samples, Lip and ProLip were spread on a plastic strip with dimensions of 0.6 cm in height and 0.5 cm in width. All samples were tested with distilled water, using both advancing and receding sequences in triplicate. The contact angle values were automatically calculated by the software.

In vitro release profile of ProLip

The release of propolis from ProLip was evaluated using the dialysis membrane technique (Weng et al., 2020). A dialysis bag (MWCO 12–14 kDa, Sigma-Aldrich, USA) was pre-soaked in distilled water for 24 h. The release medium consisted of ethanol and PBS (1:1 v/v) adjusted to pH 7.2 and degassed to remove air bubbles. Pro, Lip, and ProLip solution (5 mL) were loaded into the dialysis bag, which was then sealed and immersed in 50 mL of release medium at 37 ± 0.5 °C with continuous stirring at 600 rpm (C-MAG HS 7, IKA*). At predetermined time points (0, 0.5, 1, 2, 3, 4, 5, 6, 7, 8, 20, and 24 h), 3 mL aliquots were withdrawn and replaced with fresh medium to maintain sink conditions. Aliquots were filtered (0.22 μ m) and analysed for propolis content using UV–Vis spectrophotometry (PerkinElmer Lambda 25, UK) at 370 nm, employing the TFC method. All measurements were performed in triplicate under controlled lighting and temperature to prevent degradation. All release experiments were performed in triplicate across three independent batches.

Scanning electron microscopy (SEM)

The surface characteristics of ProLip were observed using scanning electron microscopy (SEM) (Quanta FEG 650, FEI, USA). The freeze-dried ProLip samples were mounted onto adhesive-taped stubs and sputter-coated with platinum film using an automated coater (JFC 11600) to prevent charging up by the electron beam. The SEM images were captured at various magnifications to observe the surface structure, shape, and morphological characteristics of the liposomal particles.

Attenuated total reflection fourier-transform infrared (ATR-FTIR) spectroscopy

Attenuated total reflection Fourier Transform Infrared (ATR-FTIR) spectroscopy was employed for chemical composition analysis of Pro, Lip, and ProLip (Bruker, Germany). The sample was prepared in spectroscopic grade potassium bromide (KBr) disks, and the spectra were recorded in the range of $4000-400~\rm cm^{-1}$ at a resolution of $4~\rm cm^{-1}$.

Preparation of PMA-differentiated THP-1 macrophages model

The leukemic monocyte cell line, THP-1, was retrieved from ATCC (Porton Down, Salisbury, UK). The cells were cultured in RPMI 1640 medium (Capricorn, Germany) enriched with 1% (v/v) penicillin/streptomycin (Capricorn, Germany), and 10% (v/v) FBS (Capricorn Scientific, Germany) at a seeding density of 3×10^5 cells/mL. The cells were kept at 37 °C in a humidified atmosphere with 5% CO₂. THP-1 cells were selected for this study due to their reproducible differentiation into macrophage-like cells, well-characterized response profiles, and suitability for controlled in vitro assays, allowing reliable investigation of immune-modulatory mechanisms^{85,101}. For differentiation, the cells were treated with PMA (Sigma-Aldrich, USA). Briefly, 3×10^6 cells/mL of cells were seeded in a T-25 plate and induced for 48 h by PMA (60 ng/mL). After differentiation, cells were rested for another 24 h before being subjected to further assays.

Measurement of cytokine production

To investigate the ability of ProLip on the production of tumor necrosis factor-α (TNF-α), interleukin-6 (IL-6), IL-10, and IL-1ß in the human macrophage model, cells were co-stimulated with lipopolysaccharide (LPS) (Sigma-Aldrich, USA) at 500 ng/mL. The level of secreted TNF-α, IL-6, IL-10, and IL-1ß were measured using a commercial ELISA kit (ElabScience Biotechnology Co., Ltd, China). Absorbance was recorded at 450 nm using a microplate reader, with a wavelength correction at 550 nm. Cytokine concentrations were determined by comparing the absorbance values to a standard curve.

Transmission electron microscopy (TEM) analysis of THP-1 macrophages

Macrophage morphology was observed by transmission electron microscopy (TEM). The cell pellets were fixed in McDowell-Trump fixative overnight and post-fixed with 1% osmium tetroxide for 1 h at room temperature. After washing thoroughly, the cells were dehydrated using a series of graded ethanol solutions (50%, 70%, and 95%) for 15 min each, followed by 30 min in 100% ethanol. Cells were further dehydrated using 100% acetone for 10 min, and then infiltrated overnight with a 1:1 mixture of acetone and Spurr's resin. Subsequently, the cells were further infiltrated with a fresh change of pure Spurr's resin for 3 days and embedded in pure Spurr's resin at 60 °C overnight. Specimen blocks were ultrathin-sectioned using a PowerTome XL ultramicrotome (RMC Boeckeler Instruments, Inc., Tucson, Arizona, USA) with an Ultra 45 Diatome diamond knife (Diatome, Biel, Switzerland), producing sections of 70–90 nm. The sections were collected on copper grids and stained with

uranyl acetate and lead citrate, then imaged using energy-filtered transmission electron microscopy (EFTEM) on a Libra 120 (Carl Zeiss Meditec AG, Jena, Germany).

In vitro adjuvant activity of macrophages with breast cancer cells

Three separate assays were conducted, including the apoptosis assay, scratch wound assay, and Transwell invasion assay. First, MCF-7 cells were obtained from American Type Culture Collection (ATCC $^{\circ}$, HTB-22 $^{\infty}$) and were authenticated by ATCC using PCR amplification and restriction digestion prior to distribution. Cells were cultured in high-glucose DMEM (Capricorn Scientific, Germany) supplemented with 10% (v/v) FBS and 1% (v/v) penicillin/streptomycin at 37 $^{\circ}$ C in a humidified 5% CO₂ incubator. Cells were used within 15 passages from the original ATCC vial to minimize genetic drift. Cultures were routinely monitored for mycoplasma contamination by microscopic observation of morphology and growth characteristics, with no contamination detected. MCF-7 cells (1×10 6 /mL) were seeded into a T-25 culture flask and allowed to adhere for 24 h. Then, cells were treated for another 24 h with macrophage conditioned media treated with Pro, ProLip, Pro+LPS, ProLip+LPS, LPS, and doxorubicin. Apoptosis was assessed by flow cytometry using Annexin V and propidium iodide (PI) co-staining.

For the scratch wound assay, MCF-7 cells were scratched and then incubated for 24 h to observe the change in the wounded area. Images of the cells were captured using an inverted microscope, and the healed area was quantified using Image J software (version 1.54 g, National Institute of Health, USA).

As for the Transwell invasion assay, THP-1 cells were seeded into the lower compartment of a 6-well plate, followed by differentiation. After the differentiation was completed, MCF-7 cells $(5 \times 10^5 \text{ cells per well})$ were seeded onto the upper inserts. The assay was carried out for 24 h. After the incubation period, the invasive cells that passed through the membrane to the lower compartment were fixed in 100% methanol (Sigma-Aldrich, St. Louis, USA) for 20 min. After re-washing with PBS and air drying, chambers were photographed under an inverted microscope at 20 × magnification for five random fields per insert. The percentage of invaded cells was calculated by Image J software (version 1.54 g, National Institute of Health, USA).

Statistical analysis

Data were expressed as means ± standard deviation (SD) and analysed using one-way analysis of variance (ANOVA) to compare the differences among the groups, followed by Tukey's test as the post hoc test. A p-value of <0.05 was considered statistically significant. Statistical analysis was performed using the SPSS software package (version 20.0, SPSS, Chicago, IL, USA), and graphs were created using Microsoft Excel.

Data availability

Data is provided within the manuscript or supplementary information files.

Received: 4 June 2025; Accepted: 10 September 2025

Published online: 15 October 2025

References

- 1. Khan, M., Maker, A. V. & Jain, S. The evolution of cancer immunotherapy. Vaccines 9, (2021).
- 2. Garg, P. et al. Next-generation immunotherapy: advancing clinical applications in cancer treatment. J. Clin. Med. 13, (2024).
- 3. Gupta, S. L., Basu, S., Soni, V. & Jaiswal, R. K. Immunotherapy: an alternative promising therapeutic approach against cancers. Mol. Biol. Rep. 49, 9903–9913 (2022).
- Mantovani, A., Allavena, P., Marchesi, F. & Garlanda, C. Macrophages as tools and targets in cancer therapy. Nat. Rev. Drug Discov. 21, 799–820 (2022).
- DeNardo, D. G. & Ruffell, B. Macrophages as regulators of tumour immunity and immunotherapy. Nat. Rev. Immunol. 19, 369–382 (2019).
- Abdullah, N. A. et al. Phytochemicals, mineral contents, antioxidants, and antimicrobial activities of propolis produced by Brunei stingless bees Geniotrigona thoracica, heterotrigona itama, and tetrigona Binghami. Saudi J. Biol. Sci. 27, 2902–2911 (2020).
- 7. Lim, J. R., Chua, L. S. & Dawood, D. A. S. Evaluating biological properties of stingless bee propolis. Foods 12, (2023).
- 8. Phuong, D. T. L. et al. Chemical constituents, cytotoxicity, and molecular docking studies of *Tetragonula iridipennis* propolis. *Nat. Prod. Commun.* 18, (2023).
- Mahmad, A., Chua, L. S., Noh, T. U., Siew, C. K. & Seow, L. J. Harnessing the potential of heterotrigona Itama propolis: an overview of antimicrobial and antioxidant properties for nanotechnology–Based delivery systems. *Biocatal. Agric. Biotechnol.* 54, 102946 (2023).
- 10. Mubarak, A., Maslim, S. M., Lob, S., Anuar, M. N. N. & Abd Razak, S. B. Efficacy of stingless bee (*Heterotrigona itama*) propolis aqueous extract in controlling anthracnose and maintaining postharvest quality of Chilli (*Capsicum annuum*) during storage. *Int. FOOD Res. J.* 30, 375–385 (2023).
- 11. Emil, A. B. et al. Propolis extract nanoparticles alleviate diabetes-induced reproductive dysfunction in male rats: antidiabetic, antioxidant, and steroidogenesis modulatory role. Sci. Rep. 14, 30607 (2024).
- 12. Tavares, L. et al. Encapsulation and application in the food and pharmaceutical industries. *Trends Food Sci. Technol.* **127**, 169–180 (2022).
- 13. Saroglu, O. & Karadag, A. Propolis-loaded liposomes: characterization and evaluation of the in vitro bioaccessibility of phenolic compounds. *ADMET DMPK*. **12**, 209–224 (2024).
- 14. Rudžińska, M., Grygier, A., Knight, G. & Kmiecik, D. Liposomes as carriers of bioactive compounds in human nutrition. *Foods* 13. (2024). https://doi.org/10.3390/foods13121814
- Zhang, X. et al. Application of lipopolysaccharide in Establishing inflammatory models. Int. J. Biol. Macromol. 279, 135371 (2024).
- 16. Chen, C., Yan, W., Tao, M. & Fu, Y. NAD(+) metabolism and immune regulation: new approaches to inflammatory bowel disease therapies. *Antioxidants (Basel Switzerland)* 12, (2023).
- 17. Sahoo, P. K., Ravi, A., Liu, B., Yu, J. & Natarajan, S. K. Palmitoleate protects against lipopolysaccharide-induced inflammation and inflammasome activity. *J. Lipid Res.* 65, 100672 (2024).
- 18. Wijdan, S. A., Bokhari, S. M. N. A., Alvares, J. & Latif, V. The role of interleukin-1 beta in inflammation and the potential of immune-targeted therapies. *Pharmacol. Res. Rep.* **3**, 100027 (2025).

- 19. Wyczanska, M. et al. Interleukin-10 enhances recruitment of immune cells in the neonatal mouse model of obstructive nephropathy. Sci. Rep. 14, 5495 (2024).
- Murakami, M., Kamimura, D. & Hirano, T. Pleiotropy and specificity: insights from the Interleukin 6 family of cytokines. *Immunity* 50, 812–831 (2019).
- 21. Aliyu, M. et al. Interleukin-6 cytokine: an overview of the immune regulation, immune dysregulation, and therapeutic approach. *Int. Immunopharmacol.* **111**, 109130 (2022).
- 22. Moreno-Mendieta, S. et al. Understanding the phagocytosis of particles: the key for rational design of vaccines and therapeutics. *Pharm. Res.* **39**, 1823–1849 (2022).
- 23. Eustaquio, T. et al. Electron microscopy techniques employed to explore mitochondrial defects in the developing rat brain following ketamine treatment. Exp. Cell. Res. 373, 164–170 (2018).
- 24. Youn, D. H. et al. Mitochondrial dysfunction associated with autophagy and mitophagy in cerebrospinal fluid cells of patients with delayed cerebral ischemia following subarachnoid hemorrhage. Sci. Rep. 11, 16512 (2021).
- 25. Lancaster, C. E. et al. Phagosome resolution regenerates lysosomes and maintains the degradative capacity in phagocytes. *J. Cell. Biol.* 220, (2021).
- 26. Greene, C. J. et al. Macrophages disseminate pathogen associated molecular patterns through the direct extracellular release of the soluble content of their phagolysosomes. *Nat. Commun.* 13, 3072 (2022).
- 27. Hipolito, V. E. B. et al. Enhanced translation expands the endo-lysosome size and promotes antigen presentation during phagocyte activation. *PLoS Biol.* 17, e3000535 (2019).
- 28. Buratta, S. et al. Lysosomal exocytosis, exosome release and secretory autophagy: The autophagic- and endo-lysosomal systems go extracellular. *Int. J. Mol. Sci.* 21. https://doi.org/10.3390/ijms21072576 (2020).
- 29. Nsairat, H. et al. Liposomes: structure, composition, types, and clinical applications. Heliyon 8, e09394 (2022).
- Marrocco, A. & Ortiz, L. A. Role of metabolic reprogramming in pro-inflammatory cytokine secretion from LPS or silicaactivated macrophages. Front. Immunol. 13, 936167 (2022).
- 31. Yan, G. et al. Membrane ruffles: composition, function, formation and visualization. *Int. J. Mol. Sci.* **25**, (2024).
- 32. Lillico, D. M. E., Pemberton, J. G. & Stafford, J. L. Selective regulation of cytoskeletal dynamics and filopodia formation by teleost leukocyte immune-type receptors differentially contributes to target capture during the phagocytic process. *Front. Immunol.* 9, (2018).
- Cornell, C. E. et al. Target cell tension regulates macrophage trogocytosis. BioRxiv Prepr Serv. Biol. https://doi.org/10.1101/2024. 12.02.626490 (2024).
- 34. Javed, S., Mangla, B. & Ahsan, W. From propolis to nanopropolis: an exemplary journey and a paradigm shift of a resinous substance produced by bees. *Phyther Res.* **36**, 2016–2041 (2022).
- 35. Suhandi, C. et al. Propolis-Based nanostructured lipid carriers for α-mangostin delivery: formulation, characterization, and in vitro antioxidant activity evaluation. *Molecules* **28**, (2023).
- 36. Saddiqi, M. E., Kadir, A., Abdullah, A., Abu Bakar Zakaria, F. F. J., Banke, I. S. & M. Z. & Preparation, characterization and in vitro cytotoxicity evaluation of free and liposome-encapsulated Tylosin. *OpenNano* 8, 100108 (2022).
- 37. Fulton, M. D. & Najahi-Missaoui, W. Liposomes in cancer therapy: how did we start and where are we now. *Int. J. Mol. Sci.* 24, (2023).
- 38. Chen, J. et al. Recent advances and clinical translation of liposomal delivery systems in cancer therapy. Eur. J. Pharm. Sci. 193, 106688 (2024).
- 39. Kustiawan, P. M., Syaifie, P. H., Khairy Siregar, A., Ibadillah, K. A., Mardliyati, E. & D. & New insights of propolis nanoformulation and its therapeutic potential in human diseases. *ADMET DMPK.* 12, 1–26 (2024).
- 40. Hossain, R. et al. Propolis: an update on its chemistry and Pharmacological applications. Chin. Med. 17, 100 (2022).
- 41. Haripriyaa, M. & Suthindhiran, K. Pharmacokinetics of nanoparticles: current knowledge, future directions and its implications in drug delivery. *Futur J. Pharm. Sci.* **9**, 113 (2023).
- 42. Baranov, M. V., Kumar, M., Sacanna, S. & Thutupalli, S. Bogaart, G. Modulation of immune responses by particle size and shape. *Front. Immunol.* 11, 607945 (2020). van den.
- Lohcharoenkal, W., Wang, L., Chen, Y. C. & Rojanasakul, Y. Protein nanoparticles as drug delivery carriers for cancer therapy. Biomed. Res. Int. 2014 180549 (2014).
- 44. Disalvo, A. & Frias, M. A. Surface characterization of lipid biomimetic systems. *Membranes (Basel)* 11, (2021).
- 45. Németh, Z. et al. Quality by design-driven zeta potential optimisation study of liposomes with charge imparting membrane additives. *Pharmaceutics* 14, (2022).
- Kelly, C., Jefferies, C. & Cryan, S. A. Targeted liposomal drug delivery to monocytes and macrophages. J. Drug Deliv. 2011 727241 (2011).
- Ceylan, S. Propolis loaded and genipin-crosslinked pva/chitosan membranes; characterization properties and cytocompatibility/ genotoxicity response for wound dressing applications. *Int. J. Biol. Macromol.* 181, 1196–1206 (2021).
- 48. Bakhtiary, S. et al. Culture and maintenance of neural progressive cells on cellulose acetate/graphene–gold nanocomposites. *Int. J. Biol. Macromol.* **210**, 63–75 (2022).
- 49. Lamour, G. et al. Contact angle measurements using a simplified experimental setup. J. Chem. Educ. 87, 1403-1407 (2010).
- Ramli, N. A., Ali, N. & Hamzah, S. Yatim, N. I. Physicochemical characteristics of liposome encapsulation of stingless bees' propolis. Heliyon 7, e06649 (2021).
- 51. Silveira, M. A. D. et al. Efficacy of Brazilian green propolis (EPP-AF) as an adjunct treatment for hospitalized COVID-19 patients: A randomized, controlled clinical trial. *Biomed. Pharmacother.* **138**, 111526 (2021).
- 52. Zamarrenho, L. G. et al. Effects of three different Brazilian green propolis extract formulations on pro- and anti-inflammatory cytokine secretion by macrophages. Appl. Sci. 13 (2023). https://doi.org/10.3390/app13106247
- 53. Ross, E. A., Devitt, A., Johnson, J. R. & Macrophages the good, the bad, and the gluttony. Front. Immunol. 12, (2021).
- 54. Bachiega, T. F., Orsatti, C. L., Pagliarone, A. C. & Sforcin, J. M. The effects of propolis and its isolated compounds on cytokine production by murine macrophages. *Phyther Res.* 26, 1308–1313 (2012).
- 55. Wang, K. et al. Polyphenol-rich propolis extracts from China and Brazil exert anti-inflammatory effects by modulating ubiquitination of TRAF6 during the activation of NF-κB. *J. Funct. Foods.* **19**, 464–478 (2015).
- 56. Alqarni, A. M. et al. Propolis exerts an anti-inflammatory effect on PMA-differentiated THP-1 cells via inhibition of purine nucleoside phosphorylase. *Metabolites* **9**, (2019).
- 57. Barnabei, L., Laplantine, E., Mbongo, W., Rieux-Laucat, F. & Weil, R. NF-κB: at the borders of autoimmunity and inflammation. *Front. Immunol.* **12**, 716469 (2021).
- 58. Zhang, T., Ma, C., Zhang, Z., Zhang, H. & Hu, H. NF-κB signaling in inflammation and cancer. MedComm 2, 618–653 (2021).
- 59. Yu, H., Lin, L., Zhang, Z., Zhang, H. & Hu, H. Targeting NF-κB pathway for the therapy of diseases: mechanism and clinical study. Signal. Transduct. Target. Ther. 5, 209 (2020).
- 60. Mulero, M. C., Huxford, T., Ghosh, G. & NF-κB, I. B. and IKK: Integral components of immune system signaling. In *Structural Immunology* (eds Jin, T. & Yin, Q.). https://doi.org/10.1007/978-981-13-9367-9_10. (Springer, 2019).
- Adli, M., Merkhofer, E., Cogswell, P. & Baldwin, A. S. IKKα and IKKβ each function to regulate NF-κB activation in the TNF-Induced/Canonical pathway. PLoS One. 5, e9428 (2010).
- 62. Mao, H., Zhao, X. & Sun, S. NF-κB in inflammation and cancer. Cell. Mol. Immunol. 22, 811-839 (2025).

- 63. Herrington, F. D., Carmody, R. J. & Goodyear, C. S. Modulation of NF-κB signaling as a therapeutic target in autoimmunity. SLAS Discov. 21, 223–242 (2016).
- 64. Khan, A., Zhang, Y., Ma, N., Shi, J. & Hou, Y. NF-κB role on tumor proliferation, migration, invasion and immune escape. *Cancer Gene Ther.* 31, 1599–1610 (2024).
- 65. Almowallad, S., Alqahtani, L. S. & Mobashir, M. NF-kB in signaling patterns and its temporal dynamics encode/decode human diseases. *Life (Basel Switzerland)* 12, (2022).
- Pavitra, E. et al. The role of NF-κB in breast cancer initiation, growth, metastasis, and resistance to chemotherapy. Biomed. Pharmacother. 163, 114822 (2023).
- 67. Abura, G. The dual role of cytokines in immunity: balancing pro-inflammatory and anti-inflammatory responses. *INOSR Appl. Sci.* 13, 28–34 (2025).
- 68. Cicchese, J. M. et al. Dynamic balance of pro- and anti-inflammatory signals controls disease and limits pathology. *Immunol. Rev.* **285**, 147–167 (2018).
- 69. Al-Qahtani, A. A., Alhamlan, F. S. & Al-Qahtani, A. A. Pro-inflammatory and anti-inflammatory interleukins in infectious diseases: A comprehensive review. *Trop. Med. Infect. Dis.* **9**, (2024).
- Luo, Y. & Zheng, S. G. Hall of fame among Pro-inflammatory cytokines: Interleukin-6 gene and its transcriptional regulation mechanisms. Front. Immunol. 7, 604 (2016).
- Iyer, S. S. & Cheng, G. Role of Interleukin 10 transcriptional regulation in inflammation and autoimmune disease. Crit. Rev. Immunol. 32, 23–63 (2012).
- 72. Mankan, A. K., Lawless, M. W., Gray, S. G., Kelleher, D. & McManus, R. NF-kappaB regulation: the nuclear response. J. Cell. Mol. Med. 13, 631–643 (2009).
- 73. Al-Hariri, M. Immune's-boosting agent: Immunomodulation potentials of propolis. J. Family Community Med. 26, 57-60 (2019).
- 74. Takikawa, M., Fujisawa, M., Yoshino, K. & Takeoka, S. Intracellular distribution of lipids and encapsulated model drugs from cationic liposomes with different uptake pathways. *Int. J. Nanomed.* 8401–8409 (2020).
- 75. Gandek, T. B., van der Koog, L. & Nagelkerke, A. A comparison of cellular uptake mechanisms, delivery efficacy, and intracellular fate between liposomes and extracellular vesicles. *Adv. Healthc. Mater.* 12, 2300319 (2023).
- de Almeida, M. S. et al. Understanding nanoparticle endocytosis to improve targeting strategies in nanomedicine. *Chem. Soc. Rev.* 50, 5397–5434 (2021).
- Yang, F., Teves, S. S., Kemp, C. J., Henikoff, S. & Doxorubicin DNA torsion, and chromatin dynamics. *Biochim. Biophys. Acta.* 1845, 84–89 (2014).
- Szondy, Z., Sarang, Z., Kiss, B., Garabuczi, É. & Köröskényi, K. Anti-inflammatory mechanisms triggered by apoptotic cells during their clearance. Front. Immunol. 8, 909 (2017).
- 79. Aminin, D. & Wang, Y. M. Macrophages as a 'weapon' in anticancer cellular immunotherapy. *Kaohsiung J. Med. Sci.* **37**, 749–758 (2021).
- 80. Shen, J. et al. Anti-cancer therapy with TNFα and IFNγ: A comprehensive review. Cell. Prolif. 51, e12441 (2018).
- 81. Wei, S. Hormone receptors in breast cancer: an update on the uncommon subtypes. Pathol. Res. Pract. 250, 154791 (2023).
- 82. Xiong, X. et al. Breast cancer: pathogenesis and treatments. Signal. Transduct. Target. Ther. 10, 49 (2025).
- 83. Kim, N. & Lukong, K. E. Treating ER-positive breast cancer: a review of the current FDA-approved serms and SERDs and their mechanisms of action. *Oncol. Rev.* **19–2025**, (2025).
- 84. Hopkinson, B. M. et al. Establishment of a normal-derived Estrogen receptor-positive cell line comparable to the prevailing human breast cancer subtype. *Oncotarget* 8, 10580–10593 (2017).
- 85. Mohd Yasin, Z. N., Idrus, M., Hoe, F. N., Yvonne-Tee, G. B. & C. H. & Macrophage polarization in THP-1 cell line and primary monocytes: A systematic review. *Differentiation* 128, 67–82 (2022).
- Phuphanitcharoenkun, S. et al. Characterization of macrophages associated with human skin models exposed to UV radiation. Commun. Biol. 7, 1284 (2024).
- 87. Molaaghaee-Rouzbahani, S. et al. Akkermansia muciniphila exerts Immunomodulatory and anti-inflammatory effects on gliadin-stimulated THP-1 derived macrophages. Sci. Rep. 13, 3237 (2023).
- 88. Shiratori, H. et al. THP-1 and human peripheral blood mononuclear cell-derived macrophages differ in their capacity to polarize in vitro. *Mol. Immunol.* 88, 58–68 (2017).
- 89. Chanput, W., Mes, J. J. & Wichers, H. J. THP-1 cell line: an in vitro cell model for immune modulation approach. *Int. Immunopharmacol.* 23, 37–45 (2014).
- W, C., HJ, W. & JJ, M. & The Impact of Food Bio-Actives on Gut Health: in Vitro and Ex Vivo Models (eds. KV. et al.) 147–159. https://doi.org/10.1007/978-3-319-16104-4_14 (Springer, 2015).
- 91. Franken, L., Schiwon, M. & Kurts, C. Macrophages: sentinels and regulators of the immune system. *Cell. Microbiol.* **18**, 475–487 (2016).
- 92. Luo, M., Zhao, F., Cheng, H., Su, M. & Wang, Y. Macrophage polarization: an important role in inflammatory diseases. Front. Immunol. 15, 1352946 (2024).
- 93. Atri, C., Guerfali, F. Z. & Laouini, D. Role of human macrophage polarization in inflammation during infectious diseases. *Int. J. Mol. Sci.* 19, 1801 (2018).
- 94. Shapouri-Moghaddam, A. et al. Macrophage plasticity, polarization, and function in health and disease. J. Cell. Physiol. 233, 6425–6440 (2018).
- 95. Ferenbach, D. & Hughes, J. Macrophages and dendritic cells: what is the difference? Kidney Int. 74, 5-7 (2008)
- 96. Lee, M., Du, H., Winer, D. A., Clemente-Casares, X. & Tsai, S. Mechanosensing in macrophages and dendritic cells in steady-state and disease. Front. Cell. Dev. Biol. 10, 1044729 (2022).
- 97. Muntjewerff, E. M. & Meesters, L. D. & Van Den bogaart, G. Antigen cross-presentation by macrophages. Front. Immunol. 11–2020, (2020).
- 98. Guerriero, J. L. & Macrophages Their untold story in T cell activation and function. Int. Rev. Cell. Mol. Biol. 342, 73-93 (2019).
- Guilliams, M. et al. Dendritic cells, monocytes and macrophages: a unified nomenclature based on ontogeny. Nat. Rev. Immunol. 14, 571–578 (2014).
- 100. Herdiana, Y. et al. Drug loading in chitosan-based nanoparticles. Pharmaceutics 16, (2024).
- Liu, T. et al. Optimization of differentiation and transcriptomic profile of THP-1 cells into macrophage by PMA. PLoS One. 18, e0286056 (2023).

Acknowledgements

This project was funded by the Ministry of Higher Education (MOHE), Malaysia, under the Fundamental Research Grant Scheme (FRGS) (FRGS; Reference code: FRGS/1/2021/STG01/USM/02/11), Account no. 203. CIPPT.6711976. This research was also supported by a Universiti Sains Malaysia research grant under Breast Cancer Translational Research Program (BCTRP@IPPT), Account no. 1001/CIPPT/8070033. HMZ received the Graduation Research Assistance allowance under the FRGS scheme for her postgraduate study.

Author contributions

HMZ performed the experimental work, prepared and analysed the data, and participated in the preparation of the manuscript. MM provided technical assistance with cell culture techniques. NNSNMK conceived and designed the study, secured the research grant, interpreted the data, and reviewed and edited the final draft of the manuscript. All authors have read and approved the final manuscript.

Declarations

Competing interests

The authors declare no competing interests.

Additional information

Supplementary Information The online version contains supplementary material available at https://doi.org/1 0.1038/s41598-025-19867-x.

Correspondence and requests for materials should be addressed to N.N.S.N.M.K.

Reprints and permissions information is available at www.nature.com/reprints.

Publisher's note Springer Nature remains neutral with regard to jurisdictional claims in published maps and institutional affiliations.

Open Access This article is licensed under a Creative Commons Attribution-NonCommercial-NoDerivatives 4.0 International License, which permits any non-commercial use, sharing, distribution and reproduction in any medium or format, as long as you give appropriate credit to the original author(s) and the source, provide a link to the Creative Commons licence, and indicate if you modified the licensed material. You do not have permission under this licence to share adapted material derived from this article or parts of it. The images or other third party material in this article are included in the article's Creative Commons licence, unless indicated otherwise in a credit line to the material. If material is not included in the article's Creative Commons licence and your intended use is not permitted by statutory regulation or exceeds the permitted use, you will need to obtain permission directly from the copyright holder. To view a copy of this licence, visit https://creativecommons.org/licenses/by-nc-nd/4.0/.

© The Author(s) 2025